

# Phase behavior of Cacio and Pepe sauce

G. Bartolucci,<sup>1,\*</sup> D. M. Busiello,<sup>2,3,\*</sup> M. Ciarchi,<sup>2,\*</sup> A. Corticelli,<sup>2,\*</sup> I. Di Terlizzi,<sup>2,\*</sup> F. Olmeda,<sup>4,\*</sup> D. Revignas,<sup>2,3,\*</sup> and V. M. Schimmenti<sup>2,\*</sup>

<sup>1</sup>*Department of Physics, Universitat de Barcelona, Barcelona, Spain*

<sup>2</sup>*Max Planck Institute for the Physics of Complex Systems, Dresden, Germany*

<sup>3</sup>*Department of Physics and Astronomy “G. Galilei”, University of Padova, Padova, Italy*

<sup>4</sup>*Institute of Science and Technology Austria, Am Campus 1, 3400 Klosterneuberg, Austria*

“Pasta alla Cacio e pepe” is a traditional Italian dish made with pasta, pecorino cheese, and pepper. Despite its simple ingredient list, achieving the perfect texture and creaminess of the sauce can be challenging. In this study, we systematically explore the phase behavior of Cacio and pepe sauce, focusing on its stability at increasing temperatures for various proportions of cheese, water, and starch. We identify starch concentration as the key factor influencing sauce stability, with direct implications for practical cooking. Specifically, we delineate a regime where starch concentrations below 1% (relative to cheese mass) lead to the formation of system-wide clumps, a condition determining what we term the “Mozzarella Phase” and corresponding to an unpleasant and separated sauce. Additionally, we examine the impact of cheese concentration relative to water at a fixed starch level, observing a lower critical solution temperature that we theoretically rationalized by means of a minimal effective free-energy model. Finally, we present a scientifically optimized recipe based on our findings, enabling a consistently flawless execution of this classic dish.

## I. INTRODUCTION

On several occasions, pasta has been a source of inspiration for physicists [1]. The observation that spaghetti always break up into three or more fragments, but never in two halves, puzzled even Richard Feynman himself, and the explanation of this intriguing phenomenon earned Audoly and Neukirch the Ig Nobel Prize [2]. Pasta packaging offers a natural framework to study separation upon shaking [3] and inspired the design of “morphing flat pasta” [4]. Furthermore, the deformation and swelling behavior of various pasta varieties upon cooking has been experimentally and theoretically investigated [5–8]. In particular, Hwang et al. found that the stick length of spaghetti correlates with how much the pasta is cooked, proposing an experiment to assess if pasta is “al dente” [5]. Lastly, the study of polymer rings and topological glasses has inspired a pasta prototype, a kind of closed-loop linguine that the authors have named “Anelloni” [9].

In addition to inspiring studies on its mechanical properties and structural behavior, pasta water (a mixture of starch and water) also exhibits interesting physical properties. These properties, which are central to both cooking and scientific exploration, include intriguing rheological phenomena and transitions such as non-Newtonian behavior and gelation [10]. Adding 1 part of water to 1.5–2 parts of corn starch is the most common way to get a non-newtonian fluid, sometimes called oobleck [11]. Furthermore, upon heating, the starch and water solution undergoes a gelation transition [12, 13]. Starch-enriched water can be also fundamental in stabilizing emulsions, such as in the classic “spaghetti aglio e olio” (pasta dish simply made with garlic and oil), where it helps to form a creamy sauce by preventing the formation of suspended oil droplets.

In the culinary realm, there are many other examples where the thermodynamics of mixtures plays a crucial role [14]. Phase separation often controls food texture [15], for exam-

ple in emulsions like mayonnaise, salad dressing, and other sauces [16]. In such emulsions, the homogeneous state prepared by blending or shaking the mixture is metastable and evolves towards a thermodynamic stable state composed of oily droplets, with undesired consistency. Thus, emulsions must be stabilized to remain homogeneous longer, i.e. ripening must be slowed down [17]. Delaying ripening is crucial in many other examples including chocolate [18] and the ice cream industry [19], where phase separation causes product degradation.

Moving to beverages, a famous example is the ouzo-effect, occurring during the dilution of anise-based alcohols, such as ouzo and pastis [20, 21]. When liquid water or ice is poured into these liquors, the solution becomes opaque due to the formation of oil droplets with sizes comparable to the wavelength of light. These droplets remain stable likely due to a trapping mechanism [22]. Similar droplets were recently found in limoncello, a famous Italian liquor [23].

More recently, phase separation physics has received a new wave of enthusiasm in biochemistry, caused by the discovery of phase-separated compartments in the cell cytoplasm [24, 25] and mixtures of oligomers mimicking the primordial soup [26].

Building upon the recent theoretical and experimental advances in phase separation, in this paper, we investigate the phase behavior of Cacio and pepe pasta sauce. Cacio and pepe (literally “cheese and pepper”) is a traditional recipe from Lazio, a region in central Italy. It consists of tonnarelli noodles served in a cream of pecorino cheese, pepper, and starch-enriched water, see Fig. 1 a). Its origin is commonly associated with the long travels of shepherds, who had to stuff their saddlebags with hypercaloric ingredients. Pecorino cheese was ideal due to its extraordinary shelf life, black pepper was used to stimulate heat receptors, and homemade spaghetti provided the carbohydrate intake.

Despite the short list of ingredients, preparing this dish re-

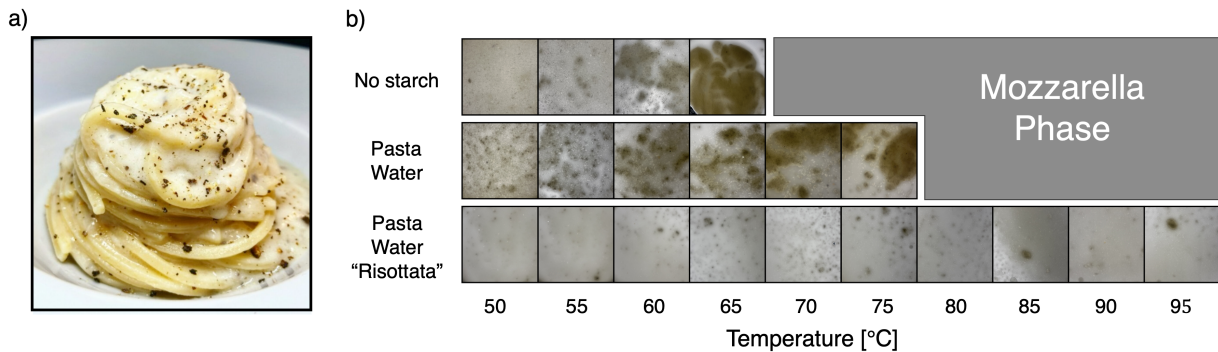


Figure 1. **Cacio and pepe pasta sauce consists of pecorino cheese, pepper and starch-enriched water** a) Tonnarelli noodles garnished with a mixture of pecorino cheese and starch-enriched water, and a sparkle of pepper. b) Snapshots of the mixture that constitutes the base for the pasta sauce, i.e. cheese and water with different amounts of starch, at different temperatures. In particular, we compare the effect of: water alone; pasta water that retains some starch (obtained by cooking 100 g of pasta in 1 liter of water); and pasta water “risottata”, i.e. pasta water heated in a pan to let the water evaporate (until reducing its total weight by three times) and starch gets concentrated. As the starch concentration increases, cheese clusters decrease in size and occur at higher temperatures. The region here named “Mozzarella phase” is characterized by huge mozzarella-like clumps of cheese suspended in water, resulting from extreme protein aggregation on heating.

quires extra care. The most delicate step is the mixing of starch-enriched water with grated cheese. One starts cooking pasta noodles in boiling water, letting them release starch, then extracts part of the water and starch solution. An essential procedure is to wait some time before mixing water and cheese, to let the water cool down. This is because, at high temperatures, cheese proteins can either form clumps upon denaturation or simply aggregate [27, 28], therefore ruining the sauce, see Fig. 1 b). But temperature is not the only physical parameter that must be carefully controlled: protein aggregation and denaturation are concentration-dependent processes, thus mixing the right amount of cheese, water, and starch is essential to avoid protein aggregates. In the absence of starch, for example, cheese in hot water forms huge clumps at a temperature around 65°C, see the first row of Fig. 1 b). If cheese is mixed with pasta water, which contains small amounts of starch, the emergence of clumps is reduced, and large protein aggregates are found at higher temperatures, see Fig. 1 b), second row. Pasta water can be “risottata”, i.e. collected and heated in a pan, so that some water evaporates and the starch is concentrated. If cheese is mixed with pasta water “risottata”, the presence of clumps is almost negligible, see the last row in Fig. 1 b).

To overcome clump formation and achieve the perfect Cacio and pepe, in this work, we characterize the phase behavior of the solution containing water, starch, and cheese, by systematically investigating the role of each one of these components. We achieve this using common kitchen tools, ensuring that our results are easily reproducible not only by scientists in the lab but also by culinary enthusiasts. The paper is organized as follows: in section II, we introduce the experimental setup and discuss the role of starch in the mixture phase phenomenology. In section III, we fix the starch percentage and vary the cheese amount. Section IV discusses a minimal theoretical model that recapitulates our experimental finding. Finally, in section V we propose a recipe for the perfect Cacio and pepe.

## II. INCREASING STARCH MITIGATES THE FORMATION OF PROTEIN CLUMPS

As discussed above, one of the most problematic aspects of making Cacio and Pepe is the appearance of large aggregates of cheese (Mozzarella phase). These clumps make the sauce inhomogeneous, giving it a gummy, unpleasant consistency. Fig. 1 b) shows how, in the absence of starch in the mixture, increasing the temperature leads to the abrupt appearance of a giant dense phase. From a culinary point of view, this represents a problem because small temperature variations can completely compromise the recipe’s outcome. The addition of pasta water, which contains small amounts of starch, mitigates the suddenness of the Mozzarella phase emergence (Fig. 1 b), second row), and increasing starch concentration even more (as in the pasta water “risottata”) suppresses the mozzarella Phase altogether (Fig. 1 b), third row). Starch thus seems to stabilize the homogeneous mixture over a large range of temperatures, allowing for less stringent temperature control during preparation.

To test this hypothesis, we conducted experiments at a fixed cheese-to-water ratio while varying the starch concentration in the water and the temperature of the system. We prepared the starch-enriched water, dissolving dry corn starch into water at ambient temperature, targeting the weight percentages shown on the bottom axis of Fig. 2 a). The mixture was heated on a stovetop to gelation, a transition marked by a noticeable increase in viscosity and opacity. Afterward, we allowed the starch-enriched water to cool to room temperature to prevent excessive heating of the cheese-water mixture during blending. Cheese and starch-enriched water were combined in equal weights and thoroughly blended with a mixer. The resulting mixture was placed in a controlled heat bath — a pot of water maintained at a constant temperature using a *sous vide* cooker device. The mixture’s temperature was further monitored with an external thermometer positioned inside it, and

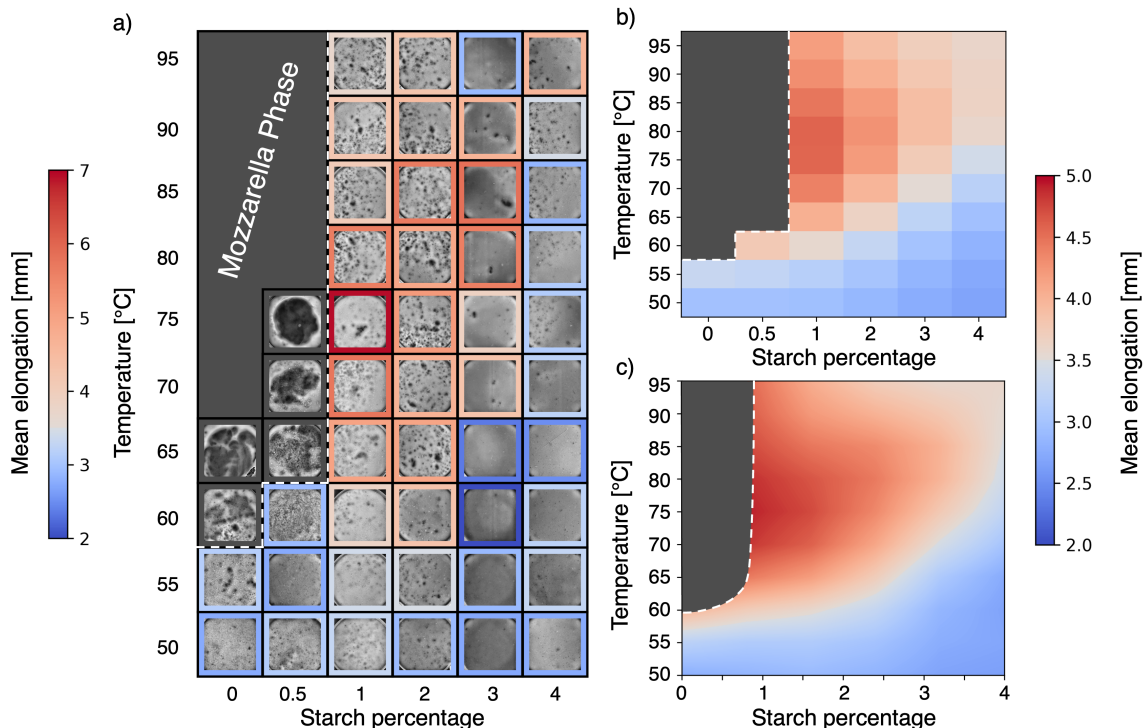


Figure 2. **Starch mitigates protein clumps.** a) Phase diagram of the sauce state as a function of the starch percentage with respect to the water and temperature in Celsius. Each box contains a snapshot of the sauce mixture taken during the experiment and its contour reflects the mean elongation of the corresponding sample via the color map shown on the left. The “mozzarella phase” indicates a region of the phase diagram where the cheese in the sample forms a clump of a size comparable to the one of the system. b) The same phase diagram as in a) is represented as a discrete heatmap with color mapping the mean elongation of the sample. c) Gaussian smoothing of the phase diagram in b).

samples were collected upon reaching thermal equilibrium, as indicated by a stable mixture temperature. Each sample was spooned onto a Petri dish and photographed. In the Supplemental Material, we report on the experimental apparatus built to heat the mixture and collect images, along with a detailed explanation of the measurement protocol. Each mixture was imaged systematically increasing the heat bath temperature by  $5^\circ\text{C}$  at each sampling and the evaporated water was replenished at each temperature step. Experiments were performed at different starch percentages to generate the images forming the phase diagram in Fig. 2 a). To characterize the mixture phase behavior, we approximated the cheese clusters as detected by quantile thresholding as ellipses and quantified their elongation in each sample (see Supplemental Material for details on data analysis). As an order parameter, we considered the mean cluster elongation since the phenomenon of protein aggregation is often referred to, in Italian kitchen jargon, as cheese “filatura”, i.e., the creation of stripes of cheese. We remark that other measures characterizing clusters’ size (or relative size) gave qualitatively similar results. Samples with larger, better separated clumps resulted in higher mean elongation values, while smoother mixtures corresponded to lower elongation values. A colored frame is used in Fig. 2 a) to associate each image to the respective value of the order parameter, measured in millimeters.

From these measurements, we constructed a phase diagram by plotting mean elongation as a function of starch concentration and temperature (see Fig.2 b)). These data were Gaussian-smoothed to create a continuous phase diagram (see Fig.2 c)). The final results reveal a clear quantitative impact of starch concentration: higher starch contents shift the transition to clumpier, less homogeneous mixtures to higher temperatures. Moreover, mixtures with low starch concentrations exhibited larger aggregate sizes, while higher starch contents reduced aggregate size and delayed clump formation. This finding corroborates the culinary insight that starch in pasta water stabilizes the Cacio and pepe sauce.

Overall, these experiments provided a quantitative picture of the starch’s role in the cheese-water mixture phase behavior. It reduces phase separation, delays the onset of clump formation to higher temperatures, and minimizes the size of aggregates, making the sauce less sensitive to mistakes in temperature control during preparation.

### III. CHEESE CONCENTRATION TUNES THE EMERGENCE OF PROTEIN CLUMPS

Having described the sauce mixture as a function of the starch, we ought to find the mixture’s degree of phase separation by varying the respective percentages of water and

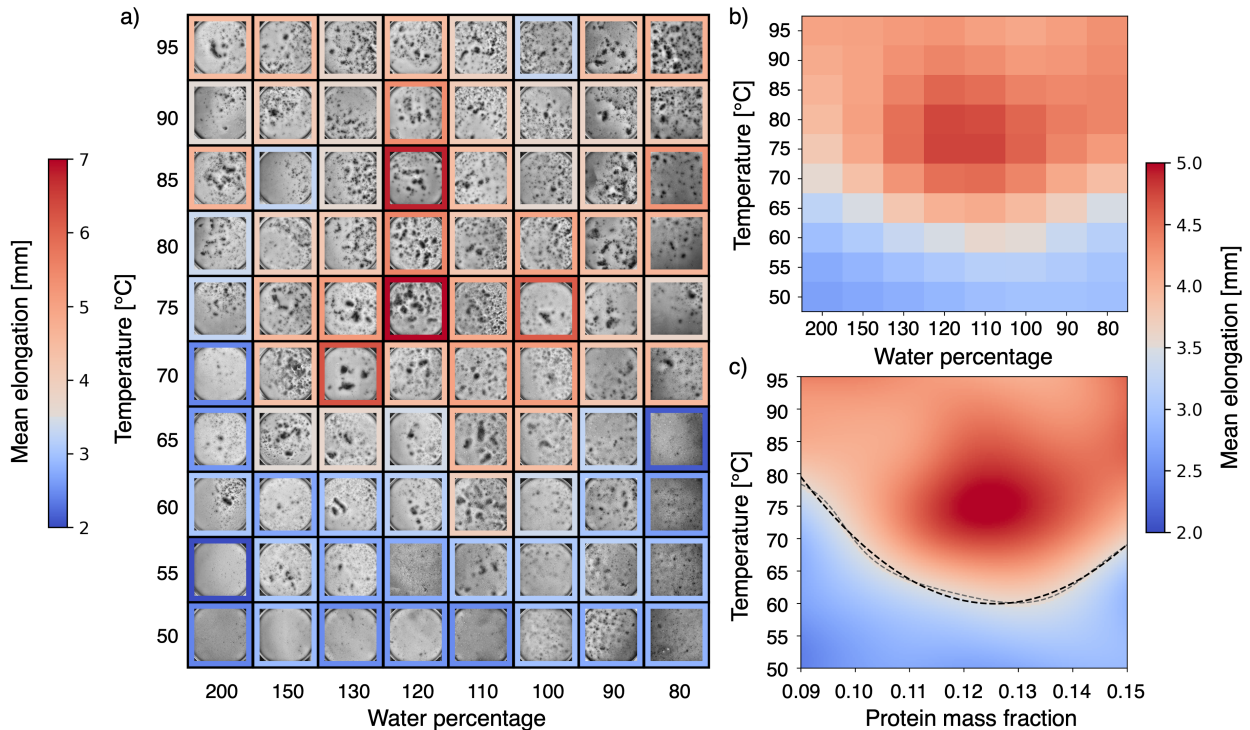


Figure 3. **Protein amount tunes aggregate formation.** a) Phase diagram of the sauce made by combining 50 g of cheese with a varying amount of starch-enriched water (here expressed as a mass percentage) as a function of the mixture temperature. The starch percentage is fixed to 1 %. Each box is colored with respect to the mean elongation of cheese clumps. b) Same phase diagram as in a), where each point is colored according to the map of the mean clump elongation. c) Phase diagram expressed as a function of protein percentage, which is the component that leads to aggregation. A Gaussian smoothing has been applied to obtain a continuous diagram. The dashed gray line indicates the isoline of median elongation, while the dashed black line represents the parabolic fit separating homogeneous from clumped domains.

cheese. To this end, we fixed the percentage of starch in the water to 1 %, a value potentially enabling the appearance of rich phase behavior. Following the procedure outlined above, we performed experiments at different percentages of starch-enriched water with respect to cheese. In Fig. 3 a), we show the resulting images, implementing a colored frame to highlight the mean elongation, the parameter employed to quantify the degree of phase separation. As expected, by fixing the concentration of starch to 1 %, we avoid the “Mozzarella phase” emerging in some of the previous experiments (see Fig. 2). From the phase diagram, we note a smooth binodal region that separates a well-mixed to a phase-separated phase, described by the mean elongation of the clumps. In Fig. 3 b), we construct a phase diagram as a function of water percentage and temperature. By obtaining the effective amount of proteins from the water percentage, in Fig. 3 c), we apply a Gaussian smoothing to obtain a continuous phase diagram as a function of protein mass fraction and temperature. This approach enables the identification of the region where clumps appear as a function of the control parameters. The binodal line separating the phase-separated domain from the homogeneous one has been identified with the isoline of mean elongation corresponding to the midpoint between the maximum and minimum observed values, after smoothing. The shape of the binodal is a paraboloid that can be fitted with a simple

quadratic functional form. The minimum of the parabola lies slightly below the protein mass fraction value 0.134, achieved with water and cheese in 1:1 proportion. A parabola with positive curvature signals that both lower and higher values of protein mass fraction correspond to well-mixed sauces even at high temperatures.

#### IV. A MINIMAL MODEL RECAPITULATES THE MIXTURE PHASE BEHAVIOR

Here, we introduce a minimal model that qualitatively matches the behavior of the mixture when the starch concentration is kept constant. Choosing which components to explicitly include in the theoretical description is a delicate step. This is because our system contains starch, salt, and lipids, together with two different kinds of proteins in the cheese, namely casein and whey (see also Fig. 4 a). Furthermore, in the range of temperatures explored, a fraction of whey proteins undergoes denaturation [29, 30]. In the following, we assume that the shape of the binodal line in the phase diagram Fig. 3 c) can be described by the phase separation of a binary mixture. We chose the binary mixture framework for its simplicity, but the applicability of such an approach has surely more limitations. In the final discussion, we outline more re-

alistic modeling approaches and their drawbacks.

As components of our model, we chose the cheese proteins (whey and casein) and an effective solvent encompassing water, starch, salt, and lipids constituting the cheese. We indicate the mass fractions of proteins and solvent with  $\phi$ , and  $\phi_s$ , respectively. Mass conservation implies  $\phi + \phi_s = 1$ . If both the components have almost equal densities, the phase diagram of a mixture in terms of the mass fraction of their components can be derived from the following free energy density

$$f = \frac{k_B T}{\nu} \left[ \frac{\phi}{n} \ln \phi + (1 - \phi) \ln(1 - \phi) + \chi \phi(1 - \phi) \right],$$

where  $\nu$  is the reference molecular mass,  $n$  indicates the relative size of cheese proteins with respect to the other components in solutions. To assess the phase behavior of the mixture, we introduce the exchange chemical potential  $\mu = n\nu \partial f / \partial \phi$  and the osmotic pressure,  $\Pi = -f + \phi \partial f / \partial \phi$ . The conditions for two phases, labelled as I and II, to stably coexist read [31]

$$\mu^I = \mu^{II}, \quad \Pi^I = \Pi^{II} \quad (1)$$

These equations have to be simultaneously solved at each temperature to determine the protein mass fraction in the coexisting phases,  $\phi^I$  and  $\phi^{II}$ . As a function of temperature,  $\phi^I$  and  $\phi^{II}$  span the binodal line observed in Fig. 3 c). Within the framework of binary mixtures, the minimum of the paraboloid-shaped binodal corresponds to a lower critical solution temperature. At this critical temperature, slightly above 60°C, the two solutions collapse, i.e.  $\phi^I = \phi^{II}$ . In principle, one has to find the right parameters  $n$  and  $\chi$  so that the binodal curve we observe is duly reconstructed by this minimal model. Notice that inferring the dependence of these parameters on temperature can be challenging. For this reason, we employ a reverse-engineering procedure, in analogy with [32]. We analytically solve Eq. (1) for  $\chi$  and  $n$  for each value of the temperature  $T$ , obtaining:

$$\chi(T) = \mathcal{F}(\phi^I, \phi^{II}) \quad n(T) = \mathcal{G}(\phi^I, \phi^{II}) \quad (2)$$

where  $\mathcal{F}$  and  $\mathcal{G}$  are specified in Eq. S1. Here,  $\phi^I$  and  $\phi^{II}$  can be directly extracted, for each value of  $T$ , from the experimental binodal in Fig. 3 c). The resulting dependence on temperature of  $\chi(T)$  (in red) and  $n(T)$  (in blue) is reported in Fig. 4 b) and constitutes the only solution for these two parameters compatible with experiments. From a microscopic point of view, an increase in the interaction parameter  $\chi$  can be due to the fact that heat induces denaturation of whey proteins, with consequential aggregation, while simultaneously favoring whey-micelle and micelle-micelle interactions [27, 28, 33] (see Fig. 4 a)). On the other hand, casein micelles are relatively heat stable, undergoing negligible dissociation on heating [34]. On the same line, the increase in the relative size might be associated with whey denaturation, or it might be due to the fact that micelle and whey proteins can form starch-mediated complexes that have a larger size [35]. Furthermore, in Fig. 4 c) we reconstruct the binodal line

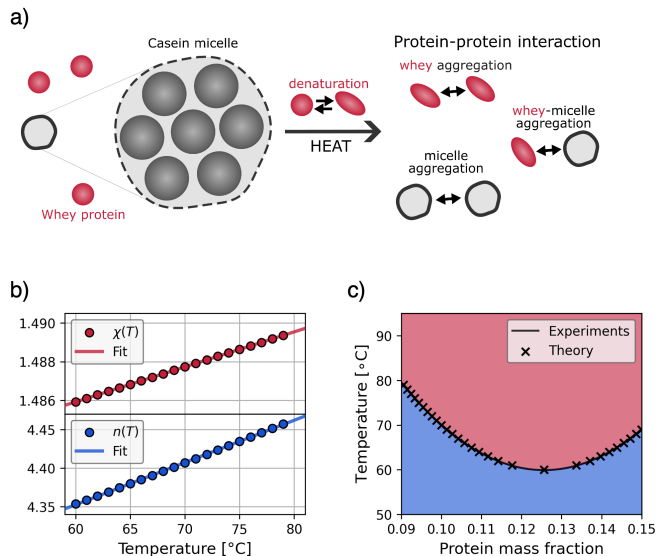


Figure 4. **A minimal model for the phase behavior of Cacio and pepe sauce.** a) Cheese is composed of casein organized in micelles together with calcium phosphate and a small percentage of whey proteins. Upon heating, whey proteins denature, reaching a state that favors whey-whey and whey-casein aggregation. Furthermore, casein micelles aggregate on heating. b) Interaction and relative size (respectively  $\chi$  and  $n$  in the effective free energy) obtained from experiments by solving Eq. (1) for different temperatures. c) Comparison between theoretical and experimental binodal curve.

employing a direct approach to Eq. (1) using the linear fits of  $\chi(T)$  and  $n(T)$  as parameters. Finally, notice that starch polymers are roughly 100 times larger than proteins while being 100 times less abundant in solution. As a consequence, we expected a relative size of the order of (or slightly greater than) the unity. This expectation is confirmed by our analysis, hinting at the fact that our model, despite its simplicity, is able to capture the main features of the observed phase behaviour.

## V. SCIENTIFIC RECIPE

A true Italian grandmother or a skilled home chef from Rome would never need a scientific recipe for Cacio and pepe, relying instead on instinct and years of experience. For everyone else, this guide offers a practical way to master the dish. Preparing Cacio and pepe successfully depends on getting the balance just right, particularly the ratio of starch to cheese. The concentration of starch plays a crucial role in keeping the sauce creamy and smooth, without clumps or separation. If the starch content is less than 1% of the cheese weight, the sauce is prone to separating into unpleasant system-sized clumps corresponding to the “mozzarella phase” in Figures 1 and 2. On the other hand, exceeding 4% starch results in a sauce that becomes stiff and unappetizing as it cools. The ideal range, as confirmed by both taste and texture tests, lies between 2% and 3%, ensuring stability and a pleasant consistency.

For a practical example, consider preparing Cacio and pepe for two hungry people. This typically requires 240 grams of pasta (tonnarelli is preferred, though spaghetti or rigatoni also works well) and 160 grams of cheese. Traditionalists would insist on using only pecorino, but some argue that up to 30% Parmesan is acceptable, though this remains a point of debate. To achieve the correct starch ratio, 4 grams of starch is optimal for 160 grams of cheese.

The pasta water alone does not contain enough starch to stabilize the sauce effectively. As we already discussed, one could use pasta water “risottata”, i.e. boiled down to concentrate the starch, but the process offers little control over the final starch amount. A more precise and reliable method is to dissolve 4 grams of powdered starch (such as potato or corn starch) in 40 grams of water. Heat this mixture gently until it thickens and turns from cloudy to nearly clear. This process, known as starch gelation, increases the viscosity of the mixture. Once the starch solution is ready, allow it to cool slightly by either waiting or mixing it with a small amount of cold water. The next step is to combine the starch solution with the cheese. Manually grating the cheese is not ideal, since it leads to chunks of different sizes. We recommend blending it with the starch solution for a smooth, homogeneous sauce. If blending is difficult, add a splash of water to ease the process, and season with freshly ground black pepper to taste.

Meanwhile, cook the pasta in slightly salted water until it is al dente. Save some of the pasta cooking water before draining. Once the pasta has been drained, let it cool down for up to a minute (even a little bit longer for an amount of pasta >1kg) to prevent the heat from destabilizing the sauce. Mix the pasta with the sauce, ensuring even coating, and adjust the consistency by gradually adding reserved pasta water as needed.

One of the benefits of this stabilized sauce is its ability to withstand reheating. Unlike traditional methods that risk clumping or separation, this sauce maintains its texture and stability even when brought to temperatures in the order of 80 – 90°C. This ensures the dish can be served hot, allowing diners to enjoy it at its best.

This method offers a simple yet precise way to consistently achieve a perfect Cacio and pepe. This recipe is inspired by Luciano Monosilio’s YouTube video [36], though it does not include olive oil as suggested in his version. Despite this difference, both recipes share a focus on respecting the tradition while ensuring a reliable and enjoyable result.

## VI. DISCUSSION

In this work, we investigated the phase behavior of Cacio and pepe, one of most famous and complicated pasta recipes of Italian culinary tradition. We quantified the stabilizing role of the starch when mixed with cheese and water, which favors the homogeneity of the mixture up to temperatures in the order of water boiling point. Also, by inspecting the role of cheese protein concentration, we unveil an unforeseen binodal curve resembling the one of a phase separating system with a lower

critical solution temperature. By employing a minimal model to capture this phenomenology, we were able to extrapolate how protein-solution interaction and relative size behave as a function of temperature. Although it is difficult to map exactly our observations to the microscopies of this complex system, we rationalized these effective phenomena, shedding light on the interplay between cheese protein and starch under heating conditions, a widespread scenario in culinary experiences. Ultimately, our approach leads to the formulation of a scientific recipe for Cacio and pepe that capitalizes on our findings and highlights their applicative perspective.

A potential future direction could be to better explain the starch-dependent morphology of the dense phase. Indeed, as noticed in Figs. 1 and 2, the cheese-rich phase abruptly switches from a big clump (that we named “Mozzarella phase”) to many small clusters, as starch concentration increases. This phenomenon could be explained by using a model that explicitly considers at least three different species.

The simplest description would account for proteins in two states A and B with stronger and weaker interaction propensity, respectively, and an effective solvent encompassing water and all remaining molecules. Then one would need to account for transitions between the two states of the proteins, controlled by temperature and starch amount. In the spirit of Ref. [37], the mozzarella-like clump could represent a phase where A proteins are dominant, while small clusters could arise whenever B proteins drive phase separation. From a microscopic point of view, A proteins could correspond to denatured whey proteins, while B proteins could encompass folded whey proteins and unfolded ones sequestered by the starch. One could even include casein micelles explicitly as a fourth component, instead of incorporating them in the effective solvent. An even more detailed model could consider protein aggregates of different sizes explicitly. One then could couple phase separation and gelation, describing the switch to a mozzarella phase as the onset of a gel phase [38–40]. Such generalizations of our model could shed more light on the molecular features of this system, eventually obtaining novel insights not only into perfecting the recipe but also in the broad field of food science. However, the main issue with these multi-component approaches is that they require more experiments to derive the dependencies of all interaction and size parameters on temperature. For example, it would be necessary to quantify the fraction of denatured whey protein for each temperature in each phase, which is a hard task.

Other interesting future directions might involve a more in-depth analysis of how starch affects effective parameters and influences the viscosity of Cacio and pepe sauce, and the potential role of pepper grains, another important part of the original recipe, as aggregation nuclei. We hope this paper ignited the idea that the genuine passion for fine cuisine can be translated into insightful results to refine complex preparations and make them achievable with accessible kitchen tools.

## ACKNOWLEDGMENTS

The authors thank Frank Jülicher, for supporting the initiative and stimulating discussions. We thank Tetsuya Spippyashi for enlightening clarifications on the historical origins of Cacio and pepe and Giuseppe Ricchitelli for helping with the construction of the experimental apparatus. We further thank Martina Gaiba, Alessandro Gaiba, John D. Treado, Virginia Lepore, Eleonora Nanu, Julia Kirsch, Lara Koehler, Burak Budanur, Elizabeth Brückner, and M.J. Franco Oñate for their support and for eating up the sample leftovers.

## DATA AVAILABILITY

The data that support the findings of this study are available from the corresponding author upon reasonable request.

---

\* All authors contributed equally to this work

- [1] P. Ball, Pasta physics, *Nature Materials* **9**, 539 (2010).
- [2] B. Audoly, Fragmentation of Rods by Cascading Cracks: Why Spaghetti Does Not Break in Half, *Physical Review Letters* **95**, 10.1103/PhysRevLett.95.095505 (2005).
- [3] R. Caulkin, X. Jia, M. Fairweather, and R. A. Williams, Geometric aspects of particle segregation, *Physical Review E* **81**, 051302 (2010).
- [4] Y. Tao, Y.-C. Lee, H. Liu, X. Zhang, J. Cui, C. Mondoa, M. Babaei, J. Santillan, G. Wang, D. Luo, D. Liu, H. Yang, Y. Do, L. Sun, W. Wang, T. Zhang, and L. Yao, Morphing pasta and beyond, *Science Advances* **7**, eabf4098 (2021).
- [5] J. Hwang, J. Ha, R. Siu, Y. S. Kim, and S. Tawfick, Swelling, softening, and elastocapillary adhesion of cooked pasta, *Physics of Fluids* **34**, 042105 (2022).
- [6] N. N. Goldberg and O. M. O'Reilly, Mechanics-based model for the cooking-induced deformation of spaghetti, *Physical Review E* **101**, 013001 (2020).
- [7] K. Irie, A. K. Horigane, S. Naito, H. Motoi, and M. Yoshida, Moisture Distribution and Texture of Various Types of Cooked Spaghetti, *Cereal Chemistry* **81**, 350 (2004).
- [8] J. J. Gonzalez, K. L. Mccarthy, and M. J. Mccarthy, Textural and Structural Changes in Lasagna After Cooking, *Journal of Texture Studies* **31**, 93 (2000).
- [9] D. Michieletto and M. S. Turner, A taste for anelloni, *Physics World* **27**, 28 (2014).
- [10] L. Copeland, J. Blazek, H. Salman, and M. C. Tang, Form and functionality of starch, *Food Hydrocolloids 9th International Hydrocolloids Conference*, **23**, 1527 (2009).
- [11] V. S. R. Krishna, S. Hussain, C. R. Kiran, and K. V. Kumar, Experimental evaluation of impact energy on oobleck material (non-Newtonian fluid), *Materials Today: Proceedings International Conference on Advances in Materials Research - 2019*, **45**, 3609 (2021).
- [12] P. J. Jenkins and A. M. Donald, Gelatinisation of starch: A combined SAXS/WAXS/DSC and SANS study, *Carbohydrate Research* **308**, 133 (1998).
- [13] M. Tako, Y. Tamaki, T. Teruya, and Y. Takeda, The Principles of Starch Gelatinization and Retrogradation, *Food and Nutrition Sciences* **05**, 280 (2014).
- [14] A. J. T. M. Mathijssen, M. Lisicki, V. N. Prakash, and E. J. L. Mossige, Culinary fluid mechanics and other currents in food science, *Reviews of Modern Physics* **95**, 025004 (2023).
- [15] V. Tolstoguzov, Texturising by phase separation, *Biotechnology Advances* **24**, 626 (2006).
- [16] S. Friberg, K. Larsson, and J. Sjoblom, eds., *Food Emulsions*, 4th ed. (CRC Press, Boca Raton, 2003).
- [17] E. Dickinson, Food emulsions and foams: Stabilization by particles, *Current Opinion in Colloid & Interface Science* **15**, 40 (2010).
- [18] H. Koizumi, M. Takagi, H. Hondoh, S. Michikawa, Y. Hirai, and S. Ueno, Control of Phase Separation for CBS-Based Compound Chocolates Focusing on Growth Kinetics, *Crystal Growth & Design* **22**, 6879 (2022).
- [19] P.-A. Aichinger, C. Schmitt, D. Z. Gunes, M. E. Leser, L. Sagalowicz, and M. Michel, Phase separation in food material design inspired by Nature: Or: What ice cream can learn from frogs, *Current Opinion in Colloid & Interface Science* **28**, 56 (2017).
- [20] S. A. Vitale and J. L. Katz, Liquid Droplet Dispersions Formed by Homogeneous Liquid-Liquid Nucleation: "The Ouzo Effect", *Langmuir* **19**, 4105 (2003).
- [21] M. A. Vratsanos, W. Xue, N. D. Rosenmann, L. D. Zarzar, and N. C. Gianneschi, Ouzo Effect Examined at the Nanoscale via Direct Observation of Droplet Nucleation and Morphology, *ACS Central Science* **9**, 457 (2023).
- [22] I. Grillo, Small-angle neutron scattering study of a world-wide known emulsion: Le Pastis, *Colloids and Surfaces A: Physicochemical and Engineering Aspects* **225**, 153 (2003).
- [23] L. Chiappisi and I. Grillo, Looking into Limoncello: The Structure of the Italian Liquor Revealed by Small-Angle Neutron Scattering, *ACS Omega* **3**, 15407 (2018).
- [24] A. A. Hyman, C. A. Weber, and F. Jülicher, Liquid-Liquid Phase Separation in Biology, *Annual Review of Cell and Developmental Biology* **30**, 39 (2014).
- [25] S. F. Banani, H. O. Lee, A. A. Hyman, and M. K. Rosen, Biomolecular condensates: Organizers of cellular biochemistry, *Nature Reviews Molecular Cell Biology* **18**, 285 (2017).
- [26] G. Bartolucci, A. Calaça Serrão, P. Schwintek, A. Kühnlein, Y. Rana, P. Janto, D. Hofer, C. B. Mast, D. Braun, and C. A. Weber, Sequence self-selection by cyclic phase separation, *Proceedings of the National Academy of Sciences* **120**, e2218876120 (2023).
- [27] S. G. Anema and Y. Li, Association of denatured whey proteins with casein micelles in heated reconstituted skim milk and its effect on casein micelle size, *Journal of Dairy Research* **70**, 73 (2003).
- [28] Z. Pan, A. Ye, A. Dave, K. Fraser, and H. Singh, Kinetics of heat-induced interactions among whey proteins and casein micelles in sheep skim milk and aggregation of the casein micelles, *Journal of Dairy Science* **105**, 3871 (2022).
- [29] M. Donovan and D. Mulvihill, Thermal denaturation and aggregation of whey proteins, *Irish Journal of Food Science and Technology*, 87 (1987).
- [30] L. Zhang, R. Zhou, J. Zhang, and P. Zhou, Heat-induced denaturation and bioactivity changes of whey proteins, *International Dairy Journal* **123**, 105175 (2021).
- [31] S. A. Safran, Statistical thermodynamics of surfaces, interfaces, and membranes, CRC Press 10.1201/9780429497131 (2019).
- [32] A. W. Fritsch, A. F. Diaz-Delgado, O. Adame-Arana, C. Hoege, M. Mittasch, M. Kreysing, M. Leaver, A. A. Hyman, F. Jülicher, and C. A. Weber, Local thermodynamics govern formation and dissolution of *Caenorhabditis elegans* P granule condensates, *Proceedings of the National Academy of Sciences* **118**, e2102772118 (2021).

- [33] S. G. Anema, Heat-induced changes in caseins and casein micelles, including interactions with denatured whey proteins, *International Dairy Journal* **122**, 105136 (2021).
- [34] T. Nicolai and C. Chassenieux, Heat-induced gelation of casein micelles, *Food Hydrocolloids* **118**, 106755 (2021).
- [35] Y. Liu, Z. Tan, X. Xu, J. Liu, B. Zhu, and X. Dong, The formation of rice starch/casein complex by hydrothermal and stabilizing high internal phase emulsions with 3d printing property, *Food Hydrocolloids* **144**, 108995 (2023).
- [36] L. Monosilio, Cacio e pepe: originale vs. infallibile vs. gourmet con luciano monosilio | babish action review, YouTube (2023), available at: <https://www.youtube.com/watch?v=U4eaNqTbDDA>.
- [37] G. Bartolucci, O. Adame-Arana, X. Zhao, and C. A. Weber, Controlling composition of coexisting phases via molecular transitions, *Biophysical Journal* **120**, 4682 (2021).
- [38] J. N. Israelachvili, *Intermolecular and Surface Forces* (Academic Press, 2015).
- [39] D. Deviri and S. A. Safran, Equilibrium size distribution and phase separation of multivalent, molecular assemblies in dilute solution, *Soft Matter* **16**, 5458 (2020).
- [40] G. Bartolucci, I. S. Haugerud, T. C. Michaels, and C. A. Weber, The interplay between biomolecular assembly and phase separation, *eLife* **10.7554/elife.93003.2** (2024).

# Supplemental Material for

## Phase separation in cacio e pepe

### S1. EQUIPMENT AND EXPERIMENTAL PROTOCOL

#### Equipment

The equipment utilized in this study can be categorized into two functional components: the sauce preparation and heating system (Figures S1a and S2a), and the image acquisition system (Figures S1b and S2b).

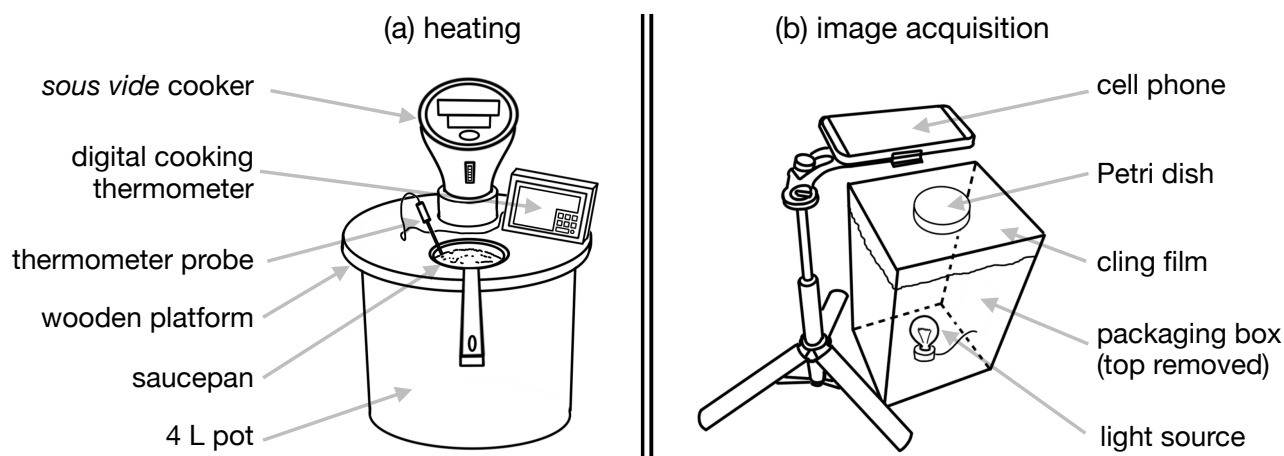


Figure S1. Scheme of the experimental equipment used in this work: (a) heating equipment, and (b) image acquisition equipment.

The sauce was prepared using standard kitchen tools, including a kitchen scale, mixing cups, an immersion blender, and spoons. The sauce heating process utilized a *sous vide* cooker in a ‘modified setting’, which included a custom-built wooden platform designed to support the cooker in the correct position and facilitate the immersion of the saucepan containing the sauce into temperature-controlled water. The hole in the wooden platform was specifically designed to serve as a constraint for the saucepan, preventing it from floating on the water of the pot, which would otherwise reduce the efficiency of heat transfer.

The image acquisition setup employed a cell phone equipped with a 12 MP f/1.6 camera (iPhone 13). The phone was mounted on a tripod positioned above a custom-made transparent support designed to hold the Petri dish containing the sauce sample. This support was constructed by removing the top portion of a cardboard packaging box and replacing it with transparent cling film, onto which the sample was deposited. A table lamp inserted through an opening at the bottom of the box served as a light source, illuminating the sample from below so that the clumps of condensed sauce appear as darker spots in the resulting images.

#### Experimental protocol

The experimental protocol we followed in this work can be summarized in the following steps:

1. **Sauce preparation:** the ingredients for a small batch of sauce ( $\approx 110$  g, with the exact weight depending on the specific formulation) are mixed in a clean mug to achieve the desired composition of cacio cheese, starch, and water. The mixture is homogenized using an immersion blender, then transferred into a saucepan and weighed. The saucepan is then placed into the wooden platform of the heating apparatus (Figure S1a).
2. **Temperature ramp:** the sauce is gradually heated up while its actual temperature of is continuously monitored using a digital cooking thermometer with a probe immersed in the sauce itself. During the heating process, the mixture is constantly stirred with a spoon to ensure uniform heating and to prevent the formation of large cheese aggregates on the saucepan walls.

When the target temperature is reached, the saucepan is promptly removed and weighed. If a detectable weight loss due to evaporation is observed (typically 1–2 g), the lost amount of water is replenished by adding the exact quantity withdrawn

from the water in the pot, which is approximately at the same temperature as the sauce. The saucepan is then returned to the platform, stirred thoroughly, and the temperature is rechecked. A slight decrease in temperature may occur due to heat dissipation during the weighing process. Once the temperature returns to the desired value (usually within a few seconds under stirring), a sample is taken from the saucepan for image acquisition. The saucepan is then weighed again to establish the reference point for the next experimental data point in the temperature ramp.

3. **Image acquisition:** the sauce sample withdrawn from the saucepan is quickly transferred into a clean Petri dish. The mixture is evenly spread across the dish by gently shaking it, and then the dish is positioned on the transparent support (Figure S1b). A photograph of the sample is captured using the cell phone. After imaging, the sauce sample is collected in a separate container for later consumption. This entire operation is optimized to be completed within approximately 20 seconds, ensuring that no significant precipitation of cheese clumps occurs during the sample's transfer and photography.
4. **Next temperature:** steps 2 and 3 are repeated for all target temperatures to construct an experimental phase diagram. The amount of sauce prepared for each batch is planned to be enough for all the measurements, with minimal leftovers at the end of the ramp (any extra is consumed afterward).

To ensure the statistical soundness of our conclusions, each temperature ramp has been replicated a minimum of twice with exactly the same control parameters.

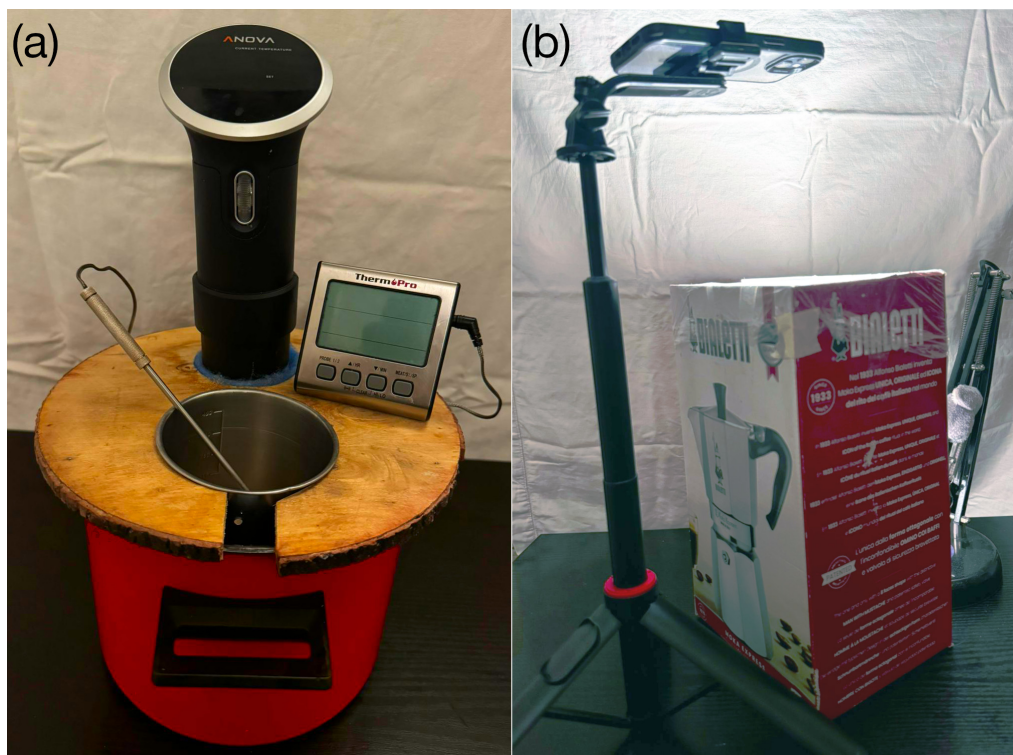


Figure S2. Photos of the actual experimental equipment used in this work: (a) heating part and (b) image acquisition part.

## S2. DATA ANALYSIS

The data analysis involved segmenting aggregates in petri dish images and computing their elongation. Initially, the images were converted to greyscale and normalized to an intensity range of  $[0, 1]$ . To enhance visibility, we adjusted exposure using the `equalize_adapthist` function from the `exposure` module in `scikit-image`, with a clip limit of 0.01. Images were then smoothed with a Gaussian filter using a sigma of 1 pixel. These parameters were determined based on iterative trials.

Next, images were cropped around the center of the petri dish to ensure uniformity in size across samples. A quantile-based segmentation was then applied. Specifically, a quantile value was selected for each sample within the interval  $[0.05, 0.25]$ . The image was binarized as

$$M_{ij} = I_{ij} < I_q,$$

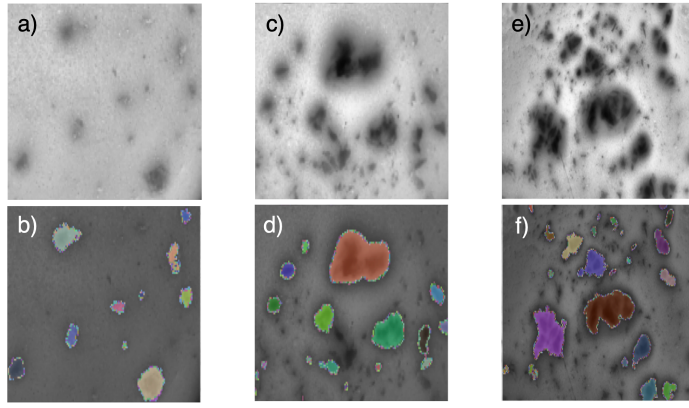


Figure S3. Three examples of segmented images illustrating varying degrees of phase separation: a, b) low, c, d) medium, and e, f) high. Panels a), c), and e) show cropped grayscale experimental images (not to scale), where darker regions represent aggregates. Corresponding segmented aggregates are displayed in panels b), d), and f), obtained using the histogram-based segmentation method described below.

where  $I_q$  is the intensity at the selected quantile  $q$ . The binary mask  $M_{ij}$  served as the seed for the watershed algorithm from `scikit-image`. For samples where aggregates formed a single large blob, the inverted image,  $1 - I_{ij}$ , was used instead.

Starting from the watershed results, we labeled the segmented regions and applied standard post-processing steps, including small object removal to address artifacts, binary dilation, hole filling, and removal of regions touching the image border.

The segmented aggregates were then analyzed using the `regionprops` routine from `scikit-image`. In particular, we reported the mean aggregate elongation in the phase diagrams, calculated using the major axis length property from `regionprops`.

To give an idea of how elongation is computed, one first calculates the covariance matrix  $C_{ab}$  for the pixel coordinates  $\{x_i, y_i\}$  of each aggregate, using the following flat measure:

$$C_{xy} = \frac{1}{N} \sum_i x_i y_i - \frac{1}{N^2} \sum_{ij} x_i y_j,$$

with analogous formulas for  $C_{xx}$  and  $C_{yy}$ . A covariance matrix carries the information of the aggregate area as  $\sqrt{\det C}$ . However, this area differs from the actual aggregate area, and so the matrix  $C_{ab}$  was scaled such that  $\det C = A^2$ , where  $A$  is the area of the segmented region. The largest eigenvalue of the rescaled  $C_{ab}$  corresponds to the square of the aggregate's elongation.

### S3. SOME ANALYTICAL FORMULAS

Here we explicitly show Eq. (2) as a function of  $\phi^I$  and  $\phi^{II}$ , namely:

$$\chi(T) = \mathcal{F}(\phi^I, \phi^{II}) = \frac{(1 + \ln(\phi^I)) \ln(1 - \phi^{II}) - (1 + \ln(1 - \phi^I)) \ln(\phi^{II}) - 2 \operatorname{Tanh}^{-1}(1 - 2\phi^I)}{2(\phi^I - \phi^{II}) + (1 - 2\phi^{II}) \ln(\phi^I) - (1 - 2\phi^I) \ln(\phi^{II})} \quad (\text{S1})$$

$$n(T) = \mathcal{G}(\phi^I, \phi^{II}) = \frac{2(\phi^I - \phi^{II}) + (1 - 2\phi^{II}) \ln(\phi^I) - (1 - 2\phi^I) \ln(\phi^{II})}{2(\phi^I - \phi^{II}) + (1 - 2\phi^{II}) \ln(1 - \phi^I) - (1 - 2\phi^I) \ln(1 - \phi^{II})} \quad (\text{S2})$$